Power-law Velocity Distributions in Granular Gases

E. Ben-Naim,[1, *] B. Machta,[2, 3, †] and J. Machta[3, ‡]

[1]*Theoretical Division and Center for Nonlinear Studies,*
Los Alamos National Laboratory, Los Alamos, New Mexico 87545
[2]*Department of Physics, Brown University, Providence, Rhode Island 02912*
[3]*Department of Physics, University of Massachusetts, Amherst, Massachusetts 01003*

The kinetic theory of granular gases is studied for spatially homogeneous systems. At large velocities, the equation governing the velocity distribution becomes linear, and it admits stationary solutions with a power-law tail, $f(v) \sim v^{-\sigma}$. This behavior holds in arbitrary dimension for arbitrary collision rates including both hard-spheres and Maxwell molecules. Numerical simulations show that driven steady-states with the same power-law tail can be realized by injecting energy into the system at very high energies. In one-dimension, we also obtain self-similar time dependent solutions where the velocities collapse to zero. At small velocities there is a steady-state and a power-law tail but at large velocities, the behavior is time-dependent with a stretched exponential decay.

I. INTRODUCTION

The statistical physics of granular gases is unusual in many ways [1–3]. Shaking a box of beads, no matter how hard, fails to generate a thermal distribution of energy. Instead, the velocity distributions are not Maxwellian [4–6] and energy may be distributed unevenly in space [7–9] or among different components of a polydisperse granular media [10, 11]. Moreover, spatial correlations may spontaneously develop [12]. Granular gases also exhibit interesting collective phenomena such as shocks [13, 14], clustering [15–19], and hydrodynamic instabilities [20, 21]. Energy dissipation, which results from inelastic collisions, is largely responsible for this rich phenomenology.

Dilute granular matter can be studied systematically using kinetic theory. This approach has been used to quantitatively model situations where the dynamics are primarily collisional [22–25]. Kinetic theory has been used to derive transport coefficients in the continuum theory of rapid granular flows, and it has also been used to model freely evolving and driven granular gases.

Spatially homogeneous systems are a natural starting point for investigations of granular gases. Theoretical, computational, and experimental studies show that the system cools indefinitely without energy injection, and that it reaches a steady-state when energy is injected to counter the dissipation. In the freely cooling case, the velocity distribution follows a self-similar form and in the forced case, the velocity distribution approaches a steady-state. In either case, the velocity distributions have sharp tails, and in particular, all of their moments are finite.

A series of recent experiments shows that for dilute and highly agitated granular systems, the velocity distri-butions have stretched exponential tails [4–6, 26]. The steady-state behavior in this regime can be accurately and quantitatively described by a spatially homogeneous kinetic theory with a spatially homogeneous thermal (white-noise) forcing. There is excellent quantitative agreement between the theoretical predictions and the experimental observations and this agreement includes statistical properties of both typical particles [26] and high-energy particles [27].

In this study, we consider the very same kinetic theory of spatially homogeneous granular gases with spatially homogeneous energy input. First, we show that in general, the tail of the velocity distribution obeys a linear equation. We then use this equation to demonstrate that stationary solutions with power-law tails are completely generic, existing for arbitrary dimension, arbitrary collision rules, and general collision rates. The characteristic exponents are obtained analytically [28].

The mechanism responsible for these stationary states is an energy cascade from large velocity scales to small velocity scales that occurs due to the inelastic particle collisions. Steady-states with the same power-law tail can be realized in driven systems where energy is injected at high energy scales. This energy injection counters the dissipation and allows the system to maintain a steady-state. We confirm these steady-states using Monte Carlo simulations. We propose that such steady states can be experimentally realized in driven granular systems in which energy is injected at large velocities, for example, by constant injection of high-energy particles into the system.

There is also a family of closely related freely cooling time-dependent states. This behavior holds in arbitrary dimension, but it is demonstrated explicitly in one dimension. In these transient states, the velocity distribution coincides with the stationary distribution up to some large velocity scale, but falls off exponentially beyond that scale. This cut-off velocity obeys Haff's cooling law and decreases algebraically with time until the power-law range collapses. The velocity distribution is self-similar and the underlying scaling function is obtained analyti-

cally using the linear Boltzmann equation. These freely cooling states are confirmed using numerical integration of the Boltzmann equation.

This paper is organized as follows. The system is set-up in section II. Dynamics of large velocities and the linear Boltzmann equation are described in section III. Stationary states are detailed in section IV, driven steady-states in section V and transient states in section VI. We conclude in section VII. An exact solution for a special case is given in the Appendix.

II. INELASTIC GASES

We study a spatially homogeneous system of identical particles undergoing inelastic collisions. In general spatial dimension, the inelastic collision rules depend on the impact angle and consequently, the theory is cumbersome. For clarity, we first describe the problem in one-dimension and then generalize the presentation to arbitrary dimension. We stress that the results in this paper hold in arbitrary dimension.

In one-dimension, the linear collision rule is

$$v_{1,2} = pu_{1,2} + qu_{2,1} \tag{1}$$

with $v_{1,2}$ the post collision velocity and $u_{1,2}$ the pre-collision velocity. To conserve momentum, the collision parameters p and q obey $p + q = 1$. The relative velocity is reduced by the restitution coefficient $r = 1 - 2p$ as follows: $(v_1 - v_2) = -r(u_1 - u_2)$. In each collision, momentum is conserved, but the total kinetic energy decreases. The energy loss is $\Delta E = pq(u_1 - u_2)^2$. Energy dissipation is maximal for the extreme case of completely inelastic collisions ($r = 0, p = 1/2$) and it vanishes for the extreme case of elastic collisions ($r = 1, p = 0$).

In this study, we consider the general collision rate

$$K(u_1, u_2) = |u_1 - u_2|^\lambda \tag{2}$$

with $0 \leq \lambda \leq 1$ the homogeneity index. For particles interacting via the central potential $U(r) \sim r^{-\nu}$, the homogeneity index is $\lambda = 1 - 2\frac{d-1}{\nu}$ [29, 30]. There are two limiting cases: (i) Hard-spheres, $\lambda = 1$, where the collision rate is linear in the velocity difference, are used to model ordinary granular media; (ii) Maxwell-molecules, $\lambda = 0$, where the collision rate is independent of the velocity are used to model granular media with certain dipole interactions [26, 31–34]. We treat the most general case $0 \leq \lambda \leq 1$ because this does not require any extra effort. By setting $\lambda = 1$ and $\lambda = 0$, one immediately obtains results for hard-spheres and Maxwell molecules, respectively.

Let $f(v, t)$ be the distribution of particles with velocity v at time t. It is normalized to unity, $\int dv f(v) = 1$ (henceforth the dependence on t is left implicit). For freely evolving and spatially homogeneous systems the distribution obeys the Boltzmann equation

$$\frac{\partial f(v)}{\partial t} = \iint du_1 du_2 |u_1 - u_2|^\lambda f(u_1) f(u_2) \tag{3}$$
$$\times \Big[\delta(v - pu_1 - qu_2) - \delta(v - u_1) \Big].$$

In this master equation, the kernel equals the collision rate (2) and the gain and loss terms simply reflect the collision law (1). The Boltzmann equation assumes perfect mixing as the probability of finding two particles at the same position is taken as proportional to the product of the individual particle probabilities. It is exact when the strong condition of perfect mixing or "molecular chaos" is met, but it is only approximate when the particle positions are correlated.

One well-known solution of the this equation is the "homogeneous cooling state" where all energy is dissipated from the system and the particles come to rest [35–37]. Thus, the system reaches a trivial stationary state, $f(v, t) \to \delta(v)$ as $t \to \infty$. Are there any nontrivial stationary solutions?

Quite surprisingly, the answer is yes. Our main result is that in arbitrary dimension and for arbitrary collision rates, including both hard spheres and Maxwell molecules, there is a family of nontrivial stationary solutions of the kinetic theory of granular gases. Moreover, there are driven steady-states that coincide with these stationary solutions.

III. CASCADE DYNAMICS

For large velocities, the nonlinear Boltzmann equation becomes linear. For clarity, we first address the one-dimensional case and then address the general dimension case. The two cases are conceptually similar but the one-dimensional case is mathematically much simpler.

A. One-Dimension

The collision integral in Eq. (3) greatly simplifies in the limit $v \to \infty$. Since the distribution decays sharply at large velocities, the product $f(u_1) f(u_2)$ is maximal when one of the pre-collision velocities is large and the other small. For the gain term there are two possibilities: either $u_1 \gg u_2$ and then $v = pu_1$ or $u_2 \gg u_1$ and then $v = qu_2$. Let us denote the large velocity by u and the small one by w. The double integral separates into two independent integrals,

$$\frac{\partial f(v)}{\partial t} = \int dw f(w) \int du \, |u|^\lambda f(u) \tag{4}$$
$$\times [\delta(v - pu) + \delta(v - qu) - \delta(u)].$$

Since $u \gg w$, the collision rate $|u - w|^\lambda$ was approximated by $|u|^\lambda$. The integral over the smaller velocity equals one,

and performing the integration over the larger velocity yields

$$\frac{\partial f(v)}{\partial t} = |v|^\lambda \left[\frac{1}{p^{1+\lambda}} f\left(\frac{v}{p}\right) + \frac{1}{q^{1+\lambda}} f\left(\frac{v}{q}\right) - f(v) \right]. \quad (5)$$

The tail of the velocity distribution satisfies a non-local but *linear* evolution equation.

The linear Boltzmann equation is valid for broader conditions compared with the full nonlinear Boltzmann equation. The only requirement is that energetic particles are uncorrelated with slower particles. This is a much weaker condition than the *"stosszahlansatz"* that the two particle density be equal to a product of one-particle densities.

Eq. (5) reflects that large velocities undergo the following cascade process

$$v \to (\, pv \, , \, qv \,), \quad (6)$$

with the rate $|v|^\lambda$. These cascade dynamics follow directly from the collision rule (1) by setting one of the incoming velocities to zero. Even though the number of particles is conserved, the number of energetic particles doubles in each cascade event (Fig. 1). Moreover, momentum is conserved but energy is dissipated in each cascade event: it is transferred from large velocities to smaller velocities.

Nearly all particles have energy proportional to some fixed energy scale but the energetic particles are very rare. As far as these energetic particles are concerned, all particles they encounter are at rest. In other words, the actual velocities of the slower particles become irrelevant. Moreover, collisions between two energetic particles are negligible. This explains why at large velocities, the nonlinear Boltzmann equation that generally concerns a collision between two particles becomes linear, that is, it concerns only one particle.

The cascade process outlined above applies only to extremely energetic particles. These particles have energy that is much larger than the typical particle energy. In what follows, we first derive the distribution of energetic particles, the tail of the distribution, and then show how to use this distribution to self-consistently obtain the typical velocity that characterizes the rest of the particles. This analysis is supplemented by numerical solution of the full nonlinear Boltzmann equation.

B. Arbitrary Dimension

We now derive the linear Boltzmann equation in general dimensions, where the collision rule is

$$\mathbf{v}_1 = \mathbf{u}_1 - (1-p)(\mathbf{u}_1 - \mathbf{u}_2) \cdot \hat{\mathbf{n}}\,\hat{\mathbf{n}}. \quad (7)$$

Here $\hat{\mathbf{n}} \equiv \mathbf{n}/n$ with $n \equiv |\mathbf{n}|$ is a unit vector parallel to the impact direction $\mathbf{n}$ (connecting the particle centers), $\mathbf{v}_{1,2}$ are the post-collision velocities, and $\mathbf{u}_{1,2}$ are the pre-collision velocities. The normal (to $\hat{\mathbf{n}}$) component of the
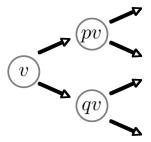

FIG. 1: The cascade process.

relative velocity is reduced by the restitution coefficient $r = 1 - 2p$ as follows, $(\mathbf{v}_1 - \mathbf{v}_2) \cdot \hat{\mathbf{n}} = -r\,(\mathbf{u}_1 - \mathbf{u}_2) \cdot \hat{\mathbf{n}}$ and the energy dissipated equals $p(1-p)|(\mathbf{u}_1 - \mathbf{u}_2) \cdot \hat{\mathbf{n}}|^2$. Similarly, the general collision rate (2) becomes $K(\mathbf{u}_1, \mathbf{u}_2) = |(\mathbf{u}_1 - \mathbf{u}_2) \cdot \hat{\mathbf{n}}|^\lambda$. The velocity distribution $f_d(\mathbf{v})$ satisfies

$$\frac{\partial}{\partial t} f_d(\mathbf{v}) = \iiint d\hat{\mathbf{n}}\, d\mathbf{u}_1\, d\mathbf{u}_2 |(\mathbf{u}_1 - \mathbf{u}_2) \cdot \hat{\mathbf{n}}|^\lambda f_d(\mathbf{u}_1) f_d(\mathbf{u}_2)$$
$$\times \; [\delta(\mathbf{v} - \mathbf{v}_1) - \delta(\mathbf{v} - \mathbf{u}_1)]. \quad (8)$$

In addition to integration over the incoming velocities, an additional integration over the impact direction is required, and this integration is normalized, $\int d\hat{\mathbf{n}} = 1$. The impact angle is assumed to be uniformly distributed.

The dynamics of large velocities $v \to \infty$ are simplified as in the one-dimensional case. The integration over the incoming velocities is separated into an integral over a small velocity and an integral over a large velocity $\mathbf{u}$. The former integration is immediate,

$$\frac{\partial}{\partial t} f_d(\mathbf{v}) = \iint d\hat{\mathbf{n}}\, d\mathbf{u} |\mathbf{u} \cdot \hat{\mathbf{n}}|^\lambda f_d(\mathbf{u}) \times \quad (9)$$
$$[\delta(\mathbf{v} - (1-p)\mathbf{u} \cdot \hat{\mathbf{n}}\,\hat{\mathbf{n}}) + \delta(\mathbf{v} - \mathbf{u} + (1-p)\mathbf{u} \cdot \hat{\mathbf{n}}\,\hat{\mathbf{n}}) - \delta(\mathbf{v} - \mathbf{u})].$$

Let $\mu = (\hat{\mathbf{u}} \cdot \hat{\mathbf{n}})^2$; in other words, if θ is the angle between the dominant velocity and the impact angle, then $\mu = \cos^2 \theta$. There are two gain terms corresponding to the two cases $\mathbf{v} = (1-p)\mathbf{u} \cdot \hat{\mathbf{n}}\,\hat{\mathbf{n}}$ and $\mathbf{v} = \mathbf{u} - (1-p)\mathbf{u} \cdot \hat{\mathbf{n}}\,\hat{\mathbf{n}}$. These collision rules, together with the impact angle, dictate the magnitudes of the post-collision velocity in terms of the pre-collision velocity, $v = \alpha u$ and $v = \beta u$ with the following stretching parameters

$$\alpha = (1-p)\mu^{1/2}, \quad (10a)$$

$$\beta = \left[1 - (1-p^2)\mu\right]^{1/2}. \quad (10b)$$

The parameter α follows from $\hat{\mathbf{u}} = \hat{\mathbf{n}}$ and the parameter β is obtained by introducing $\mathbf{w} = \mathbf{v} - \mathbf{u}$ and then employing the collision rule $w = -\mathbf{w} \cdot \hat{\mathbf{n}} = (1-p)\mathbf{u} \cdot \hat{\mathbf{n}} = (1-p)u\mu^{1/2}$ and the identity $v^2 = u^2 + w^2 - 2uw\mu^{1/2}$. The integration over the large velocity $\mathbf{u}$ includes separate integrations over the velocity magnitude u and over the velocity direction $\hat{\mathbf{u}}$ but since this angle is a unique function of the

impact angle, the latter integration is immediate. Using the isotropic velocity distribution $f_d(\mathbf{v}) \equiv S_d v^{d-1} f(v)$ with $S_d \int dv\, v^{d-1} f(v) = 1$ and S_d the area of the d-dimensional unit hypersphere, Eq. (9) simplifies to

$$v^{d-1} \frac{\partial f(v)}{\partial t} = \iint d\hat{\mathbf{n}}\, du\, |u\mu^{1/2}|^\lambda\, u^{d-1} f(u) \qquad (11)$$
$$\times\; [\delta(v - \alpha u) + \delta(v - \beta u) - \delta(v - u)].$$

Finally, we simplify the angular integration, $d\hat{\mathbf{n}} \propto \sin^{d-2}\theta\, d\theta$. Denoting the angular integration with angular brackets $\langle g \rangle \equiv \int d\hat{\mathbf{n}}\, g(\hat{\mathbf{n}})$, we have

$$\langle g \rangle = C \int_0^1 d\mu\, g(\mu)\, \mu^{-1/2}(1-\mu)^{\frac{d-3}{2}}. \qquad (12)$$

The constant $C = 1/B(\frac{1}{2}, \frac{d-1}{2})$, with $B(a,b)$ the beta function, is set by normalization. The linear equation governing the tail of the distribution is therefore

$$\frac{\partial f(v)}{\partial t} = \left\langle v^\lambda \mu^{\lambda/2} \left(\frac{1}{\alpha^{d+\lambda}} f\left(\frac{v}{\alpha}\right) + \frac{1}{\beta^{d+\lambda}} f\left(\frac{v}{\beta}\right) - f(v) \right) \right\rangle. \qquad (13)$$

As in one-dimension, large velocities undergo the cascade process

$$v \to (\,\alpha v\,,\,\beta v\,), \qquad (14)$$

but in general dimension, the stretching parameters acquire a dependence on the impact angle. In each collision, the total velocity magnitude increases, despite the fact that the total energy decreases, as reflected by the following two inequalities

$$\alpha + \beta \geq 1, \qquad (15a)$$
$$\alpha^2 + \beta^2 \leq 1. \qquad (15b)$$

Equalities occur in the limiting cases: the total velocity magnitude is conserved in one dimension where collisions are always head-on ($\mu = 1$) and, of course, the total energy is conserved for elastic collisions ($p = 0$). Actually, a stronger statement than (15) holds: the quantity $M_s(\alpha, \beta) = \alpha^s + \beta^s - 1$ is positive for $s \leq 1$, negative for $s \geq 2$, and it may be either positive or negative in the range $1 < s < 2$, depending on the impact angle.

IV. STATIONARY SOLUTIONS

The power-law velocity distribution

$$f(v) \sim v^{-\sigma} \qquad (16)$$

is a stationary solution of the linear Boltzmann equation (5) or (13). An implicit equation for the characteristic exponent σ is obtained by inserting the power law form in the linearized Boltzmann equation and setting the time derivative to zero. In one dimension, the result is $p^{\sigma-1-\lambda} + q^{\sigma-\lambda-1} = 1$. Since the collision parameters
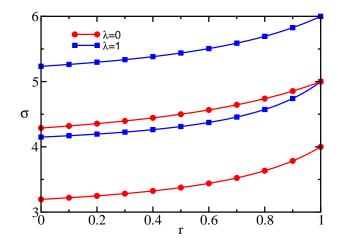

FIG. 2: The exponent σ versus the restitution coefficient r for hard-spheres ($\lambda = 1$) and Maxwell molecules ($\lambda = 0$). The top two curves are for $d = 3$ and the bottom two curves are for $d = 2$.

satisfy $p + q = 1$, the characteristic exponent in one-dimension is simply

$$\sigma = 2 + \lambda. \qquad (17)$$

Of course, the power-law behavior applies only for the tail of the distribution.

Algebraic behavior holds in arbitrary dimension. Substituting Eq. (16) into the general linear Boltzmann equation (13), the characteristic exponent is root of the equation

$$\left\langle \left(\alpha^{\sigma-d-\lambda} + \beta^{\sigma-d-\lambda} - 1 \right) \mu^{\lambda/2} \right\rangle = 0. \qquad (18)$$

This transcendental equation can be re-written explicitly in terms of the gamma function and the hypergeometric function [38]

$$\frac{1 - {}_2F_1\left(\frac{d+\lambda-\sigma}{2}, \frac{\lambda+1}{2}, \frac{d+\lambda}{2}, 1-p^2 \right)}{(1-p)^{\sigma-d-\lambda}} = \frac{\Gamma(\frac{\sigma-d+1}{2})\Gamma(\frac{d+\lambda}{2})}{\Gamma(\frac{\sigma}{2})\Gamma(\frac{\lambda+1}{2})}. \qquad (19)$$

The exponent $\sigma \equiv \sigma(d, \lambda, r)$ varies continuously with the spatial dimension d, the homogeneity index λ, and the restitution coefficient r (figure 2).

According to the bounds (15) the left hand side of Eq. (18) is positive when $\sigma - d - \lambda \leq 1$ but negative when $\sigma - d - \lambda \geq 2$. Therefore, this quantity changes sign when $1 \leq \sigma - d - \lambda \leq 2$ leading to the relatively tight bounds

$$d + 1 + \lambda \leq \sigma \leq d + 2 + \lambda. \qquad (20)$$

The lower bound (17) is realized in one-dimension where the collisions are always head-on, while the upper bound is approached, $\sigma \to d + 2 + \lambda$, in the quasi-elastic limit $r \to 1$. We note that the two limiting cases of one-dimension and elastic collisions do not commute. Moreover, the zero dissipation limit is singular: Maxwellian distributions occur when the collisions are elastic [31].

Since the energy lost in each collision is proportional to $(\Delta v)^2$ and the collision rate is proportional to $|\Delta v|^\lambda$, the energy dissipation rate is related to the following integral, $\Gamma \sim \langle v^{2+\lambda} \rangle$ where $\langle g(v) \rangle \equiv S_d \int dv\, v^{d-1} f(v) g(v)$. Hence, the bound $\sigma \leq d + 2 + \lambda$ implies that the total dissipation rate is divergent. This is a generic feature of the stationary solutions, and in fact it shows why Haff's cooling law $dT/dt = -\Gamma$, where $T = \langle v^2 \rangle$ is the granular temperature, does not apply: this rate equation assumes finite dissipation rates. In contrast, the total energy may be either finite or infinite because both $\sigma > d + 2$ and $\sigma < d+2$ are possible. The stationary states studied here appear to be fundamentally different than the infinite energy solutions of the elastic Boltzmann equation because they require dissipation and because they always involve infinite dissipation [39].

The characteristic exponent increases monotonically with the spatial dimension, the homogeneity index, and the restitution coefficient. Thus, fixing d and λ, the completely inelastic case ($r = 0$) provides a lower bound for σ with respect to r (figure 2). For hard-spheres the completely inelastic limit yields $\sigma = 4.14922$ and $\sigma = 5.23365$ in two- and three-dimensions, while for Maxwell molecules the corresponding values are $\sigma = 3.19520$ and $\sigma = 4.28807$.

The power-law behavior is in sharp contrast with the stretched exponential tails $f(v) \sim \exp(-|v|^\delta)$ that typically characterize granular gases. For freely cooling gases, $\delta = \lambda$, and for thermally forced gases, $\delta = 1+\lambda/2$ [27, 40–42]. Both behaviors immediately follow from the linear Boltzmann equation (13); in the forced case, the time derivative in (13) is replaced by the diffusive forcing term $\partial/\partial t \to D\nabla^2$. Only in the limiting case of freely cooling Maxwell molecules do power-law velocity distributions arise, but the solutions are not stationary and the characteristic exponent differs from those found here [43–46].

In what follows, we will see that such steady-states with power-law tails can be maintained by injecting energy at large velocity scales in a spatially homogeneous fashion (driven steady-state, section V). When the energy input is turned-off, the system collapses in a self-similar fashion as for freely cooling gases (time-dependent states, section VI).

V. DRIVEN STEADY-STATES

Clearly, for the system to maintain a steady-state, energy must be injected. But on the other hand, the kinetic theory above describes purely collisional dynamics: it does not contain an explicit energy injection term. In this section we show that numerical simulations of the full nonlinear equations yield steady states similar to the stationary solutions when there is a clear separation of scales between the energy injection scale V and the typical velocity scale v_0. Energy injection is limited to energies above the injection scale. Below this injection scale, there is no energy input and thus, the dynamics are
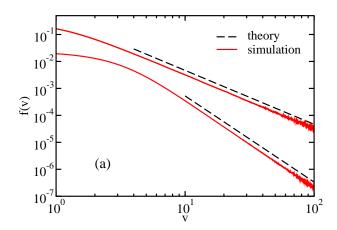

FIG. 3: The velocity distribution for Maxwell molecules in one-dimension (top curves) and in two-dimensions (bottom curves).

purely collisional and the system is described by a kinetic theory without an explicit energy source. In this sense, the driven steady-states we describe here are more fundamental than these emerging due to a thermostat, because they do not depend on the precise form of the energy injection. In other words, they are intrinsic to the collision dynamics. We note that the energy injection mechanism is not unique. We studied several concrete cases where energy is injected with a small rate at a large velocity.

The full nonlinear Boltzmann equation is solved numerically using the following direct simulation Monte Carlo technique. Collisions are simulated by selecting two particles at random with a probability proportional to the collision rate and then updating their velocities according to the collision rule (7). Energy is injected with a small rate using the following "lottery" implementation. An energy loss counter keeps track of the cumulative energy loss. With a small rate, a randomly chosen particle is "awarded" an energy equal to the reading on the loss counter. Subsequently, the loss counter is reset to zero. With this protocol, the kinetic energy remains practically constant, and moreover, energy injection occurs only at large velocity scales. For one-dimensional hard-spheres, we tested a different injection mechanism. The injection energy was drawn from a Maxwell-Boltzmann distribution with a very large energy. With a small rate, this energy was added to a randomly chosen particle.

We simulated completely inelastic Maxwell molecules and hard spheres in one- and two-dimensions starting with a uniform velocity distribution with support in the range $[-1:1]$. After a short transient, the system reaches a steady-state. In all cases, the tail of the velocity distribution decays as a power-law, and the exponent σ is in excellent agreement with the theoretical prediction, Eq. (19). Maxwell molecule simulation results are displayed in figure 3 and hard sphere simulation results in figure 4. The simulations also show that the velocity distribution is sharply suppressed beyond the injection scale.
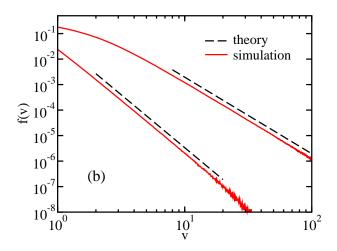
FIG. 4: The velocity distribution for hard spheres in one-dimension (top curves) and in two-dimensions (bottom curves).

The simulation results fill an important gap in our theory. Analytically, we are able to solve only the linear Boltzmann equation. The numerical simulation amounts to nothing more than a numerical solution of the full non-linear Boltzmann equation. The fact that the numerics show that the velocity distribution becomes stationary at *all* velocity scales, not just the large scales, validates the existence of the stationary solutions. An exact solution of the full Boltzmann equation for the special case of one-dimensional Maxwell molecules is detailed in the Appendix.

We conclude that the nonlinear Boltzmann equation admits stationary solutions. These solutions are certainly counterintuitive because the kinetic theory does not contain an energy injection term. Driven steady states that coincide with these stationary solutions up to some large scale can be realized by injecting energy at some large velocity scale.

We now obtain the typical velocity scale v_0 and the injection scale V as a function of the injection rate γ using scaling analysis. Clearly, if $f(v)$ is a stationary solution, so is $v_0^{-d} f(v/v_0)$ for arbitrary v_0. Let the energy injection rate (per particle) be γ and let the injection velocity be V. This scale sets an upper cutoff on the velocity distribution, beyond which the distribution should rapidly vanish. Since the system is at a steady-state, the dissipation rate

$$\Gamma \sim \langle v^{2+\lambda} \rangle \sim \int^V dv\, v^{d+1+\lambda}\, v_0^{-d} f(v/v_0) \quad (21)$$
$$\sim V^{\lambda+2}(V/v_0)^{d-\sigma},$$

must be balanced by the energy injection rate γV^2, leading to a general relation between the injection rate, the injection velocity and the typical velocity,

$$\gamma \sim V^\lambda (V/v_0)^{d-\sigma}. \quad (22)$$

The energy balance relation (22), combined with the constant energy condition $\langle v^2 \rangle \sim 1$, imposed in our simulations, yields an estimate for the typical velocity. Different behaviors emerge for finite energy and infinite energy distributions.

When $\sigma < d+2$, the constant energy constraint implies $V^{d+2-\sigma} \sim v_0^{d-\sigma}$, that combined with energy balance (22) reveals how the maximal velocity and the typical velocity scale with the injection rate

$$V \sim \gamma^{-\frac{1}{2-\lambda}}, \quad (23a)$$
$$v_0 \sim \gamma^{\frac{d+2-\sigma}{(\sigma-d)(2-\lambda)}}. \quad (23b)$$

Simulations with $d = 1$, $\lambda = 0$, and $\gamma = 10^{-4}$, are characterized by $V \approx 10^2$ and $v_0 \approx 10^{-2}$, consistent with these scaling laws.

In the complementary case, $\sigma > d + 2$, the typical velocity $v_0 \sim 1$ is set by the initial conditions because $\langle v^2 \rangle \sim v_0^2$. Energy balance (22) yields

$$V \sim \gamma^{-\frac{1}{\sigma-d-\lambda}}. \quad (24)$$

Simulations with $d = 2$, $\lambda = 1$, and $\gamma = 10^{-2}$ should be characterized by the injection scale $V \approx 50$, as in this case $\sigma \cong 4.15$. The data is consistent with this estimate.

Based on the theoretical and the simulation results, we conclude that there may be qualitative differences between the finite energy and infinite energy cases, but that fundamentally, the cases are of one nature. They represent a nonequilibrium driven steady-state where energy is injected at velocity scale V and dissipated at smaller velocities. Due to inelastic collisions, energy cascades from large velocities to small velocities. These scales are set by the injection rate and the injection protocol.

VI. TIME-DEPENDENT STATES

What happens when energy injection is turned-off? Steady-states of the type (16) can be realized only up to some upper cutoff V. In the absence of energy input, they should undergo free cooling with all energy eventually dissipated from the system.

Therefore, we anticipate that there is a time-dependent velocity cut-off $V(t)$. Below this scale the distribution is nearly the same as the stationary distribution but above this scale, the distribution has a sharp tail, analogous to the freely cooling states. Thus, the distribution is of the form $f(v,t) \equiv f(v,V)$ such that for $v < V(t)$, $f(v;V) \approx f_s(v)$ while for $v > V(t)$, the distribution decays faster than a power law. Here $f_s(v)$ is the stationary solution of the full Boltzmann equation. We set $v_0 \equiv 1$ without loss of generality.

First, consider the time dependence of the cut-off scale $V(t)$. Given the assumption that cooling occurs only through a decrease in the cut-off scale, the rate of change

of the energy is

$$\frac{dE}{dt} = \frac{d\langle v^2 \rangle}{dt} = \frac{d}{dt} \int^{V(t)} dv\, v^{d+1} f_s(v) \qquad (25)$$
$$\sim V^{d+1-\sigma} \frac{dV}{dt}.$$

The decrease in energy equals the dissipation rate $\Gamma \sim V^{d+2+\lambda-\sigma}$ from Eq. (21), showing that the cut-off velocity obeys Haff's cooling law [37],

$$\frac{dV}{dt} = -cV^{1+\lambda}. \qquad (26)$$

Therefore, the cut-off velocity decays with time as follows

$$V(t) = \left[\frac{V^{\lambda}(0)}{1 + c\lambda V^{\lambda}(0)t} \right]^{1/\lambda} \qquad (27)$$

where $V(0)$ is the initial value of the cut-off.

Since both the stationary states and free-cooling states have the same nature in one-dimension and in higher-dimensions, we expect that the time dependent states are generic as well. We describe in detail only the one-dimensional case. We seek similarity solutions of the type

$$f(v,t) \simeq f_s(v)\phi\left(\frac{v}{V}\right). \qquad (28)$$

Here, $f_s(v)$ is the stationary solution of Eq. (3) that decays as a power-law at large velocities $f_s(v) \simeq Av^{-2-\lambda}$. The cut-off function approaches unity at small arguments, $\phi(x) \to 1$ as $x \to 0$ so that the stationary solution is recovered for $v \ll V$.

A.   Linear Theory

Substituting the time dependent form (28) into the *linear* governing equation (5) yields

$$-\frac{dV/dt}{V^{1+\lambda}}\phi'(x) = x^{\lambda-1}\left[p\phi\left(\frac{x}{p}\right) + q\phi\left(\frac{x}{q}\right) - \phi(x) \right]. \qquad (29)$$

Assuming the cut-off velocity satisfies Eq. (26) with constant of proportionality c, the scaling function satisfies the linear and non-local differential equation

$$c\,\phi'(x) = x^{\lambda-1}\left[p\phi\left(\frac{x}{p}\right) + q\phi\left(\frac{x}{q}\right) - \phi(x) \right], \qquad (30)$$

with the boundary conditions $\phi(0) = 1$ and $\phi(x) \to 0$ as $x \to \infty$. Note that $\phi(x)$ must be non-analytic at $x = 0$ because all its derivatives vanish at $x = 0$ since $p + q = 1$ and $\phi(0) = 1$.

For large arguments, the last term on the right hand side dominates, and therefore, the tail of the distribution is a stretched exponential

$$\phi(x) \sim \exp\left(-C\,x^{\lambda}\right) \qquad (31)$$

with $C = (\lambda c)^{-1}$ for $\lambda > 0$. In the limiting case $\lambda = 0$ all terms on the left-hand side are comparable and the tail is algebraic: $\phi(x) \sim x^{-\sigma}$ with $c\,\sigma = 1 - p^{\sigma+1} - q^{\sigma+1}$. Thus, both the decay of the cut-off velocity and the tail behavior are as for ordinary freely cooling solutions [35]. There is, however, a difference since the distributions considered here have *two* characteristic velocities, V and v_0 and it is only the upper cut-off, V that evolves in time. After V and v_0 become comparable, the behavior crosses over to the homogeneous cooling state [35, 36] with a single characteristic velocity, v_0.

We now focus on completely inelastic hard-spheres ($p = q = 1/2$ and $\lambda = 1$) for which an exact solution is possible. Integrating Eq. (30) and imposing $\phi(0) = 1$ gives $c = (1 - p^2 - q^2) \int_0^\infty dx\, \phi(x)$, but since the cut-off scale V is defined up to a constant, we may set the integral value, $\int_0^\infty dx\, \phi(x) = 1$ leading to $c = 1 - p^2 - q^2$. When $p = q = 1/2$ then $c = 1/2$ and Eq. (30) becomes

$$\phi'(x) = 2\left[\phi(2x) - \phi(x)\right]. \qquad (32)$$

This equation can be solved using the Laplace transform $h(s) = \int dx\, e^{-sx}\phi(x)$, that satisfies the non-local equation

$$(2 + s)h(s) = 1 + h(s/2) \qquad (33)$$

with the boundary condition $h(0) = 1$ set by the normalization. Since $\phi(x) \to 1$ as $x \to 0$ then $h(s) \to s^{-1}$ as $s \to \infty$, so we make the transformation $h(s) = s^{-1}[1 - g(s)]$ with $g(0) = 1$ and $g'(0) = -1$. The auxiliary function $g(s)$ satisfies a recursion-like equation $g(s) = (1 + s/2)^{-1} g(s/2)$. Solving iteratively and invoking $g(0) = 1$, the solution is the infinite product $g(s) = \prod_{n=1}^{\infty}(1 + s/2^n)^{-1}$, and the Laplace transform is

$$h(s) = \frac{1}{s}\left(1 - \prod_{n=1}^{\infty} \frac{1}{1 + \frac{s}{2^n}} \right). \qquad (34)$$

Since the infinite product has a series of simple poles at $s = -2^{-n}$ for every integer $n \geq 1$, the scaling function is a sum of exponentials

$$\phi(x) = \sum_{n=1}^{\infty} a_n \exp\left(-2^n x\right) \qquad (35a)$$

$$a_n = \prod_{\substack{k=1 \\ k \neq n}}^{\infty} \frac{1}{1 - 2^{n-k}}, \qquad (35b)$$

with the coefficients obtained as the residues to the poles $a_n = \lim_{s \to -2^n}[(s + 2^n)h(s)]$. In contrast with freely cooling states, the scaling function $\phi(x)$ can be obtained exactly.

The Laplace transform conveniently yields the limiting behaviors of the scaling function. The simple pole closest to the origin reflects the tail behavior
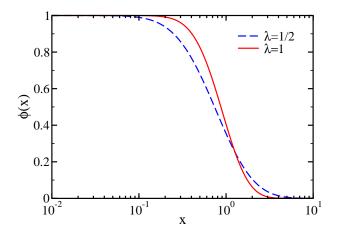
$$\phi(x) \simeq a_1 \exp(-2\,x) \qquad (36)$$

FIG. 5: The scaling function $\phi(x)$ versus x for $\lambda = 1/2$ (dashed line) and $\lambda = 1$ (solid line).
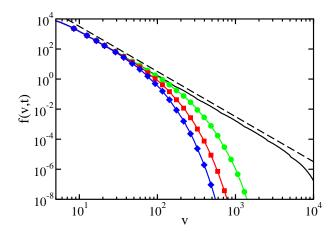

FIG. 6: The velocity distribution $f(v, t)$ versus v. Shown is the steady-state distribution before the injection is turned-off (solid line) and at three consecutive and equally-spaced later times (circles, squares, diamonds) during free cooling. Also shown for reference is a dashed line with slope -3. The velocity is in arbitrary units.

as $x \to \infty$ with $a_1 = 3.46275$ obtained from Eq. (35b). More interesting is the small x behavior, reflected by the large s behavior

$$\int_0^\infty dx \left[1 - \phi(x)\right] e^{-sx} = s^{-1} g(s) \to s^{-1} \exp\left[-C \left(\ln s\right)^2\right]$$

as $s \to \infty$ with $C = (2 \ln 2)^{-1}$. The function $g(s)$ was estimated by replacing the infinite product with a finite product

$$\prod_{n=1}^{\infty} \frac{1}{1 + \frac{s}{2^n}} \cong \prod_{n=1}^{n_*} \frac{2^n}{s} \to \exp\left[-C \left(\ln s\right)^2\right] \qquad (37)$$

with $n_* = \ln_2 s$. Inverting the log-normal Laplace transform using the steepest descent method, the leading correction to the scaling function is log-normal as well

$$1 - \phi(x) \sim \exp\left[-A \left(\ln \frac{1}{x}\right)^2\right], \qquad (38)$$

as $x \to 0$ with $A = C/4 = (8 \ln 2)^{-1}$. Thus, the scaling function is perfectly flat near the origin as all its derivatives vanish at $x = 0$ (figure 5). Physically, the small x behavior shows that there is a sizable range of velocities for which the time-dependent velocity distribution (28) coincides with the steady-state solution, $f(v, t) \simeq f_s(v)$.

The series solution (35) can be straightforwardly generalized to all $\lambda > 0$

$$\phi(x) = \sum_{n=1}^{\infty} a_n \exp\left[-(2^n x)^\lambda\right], \qquad (39a)$$

$$a_n = \prod_{\substack{k=1 \\ k \neq n}}^{\infty} \frac{1}{1 - 2^{\lambda(n-k)}}. \qquad (39b)$$

Making the transformation $y = x^\lambda$ and setting the proportionality constant $c = \lambda^{-1} 2^{-\lambda}$ such that $c = \left(1 - 2^{-\lambda}\right) \int_0^\infty dy\, \phi(y)$, Eq. (32) is generalized,

$\phi'(y) = 2^\lambda \left[\phi(2^\lambda y) - \phi(y)\right]$. Consequently, the Laplace transform is obtained from Eq. (34) by replacing 2^n with $2^{\lambda n}$, and repeating the steps leading to (35) gives (39). Figure 5 shows the scaling function for $\lambda = 1/2$. As λ decreases the cut-off becomes less sharp and the flat region near $x = 0$ less broad.

In summary, we find that there are time-dependent states associated with the steady states. In these transient states, the velocity distribution is characterized by a cut-off velocity scale that decays with time according to Haff's law. Below this velocity, the energy cascade is unaffected and the velocity distribution agrees with the stationary distribution but above this scale, the distribution is exponentially suppressed. We relied only on the linear Boltzmann equation to derive a scaling form for the cut-off function. Of course, the full nonlinear equation (3) is still relevant as it governs the dynamics of small velocities via the stationary solution $f_s(v)$. This guarantees that the velocity distribution is properly normalized, and specifically, that the integral over small velocities remains finite.

B. Numerical Simulations

We numerically integrated the hard-sphere Boltzmann equation in one-dimension to verify that the predictions of the previous subsection hold for the full non-linear dynamics. Velocity bins are kept, each with a double precision number representing the number of particles within that velocity range. In the simulation, two velocity bins are chosen randomly with a rate proportional to the collision rate. When two bins "collide", particles are transferred from each into target bins, determined by the collision rule (1).

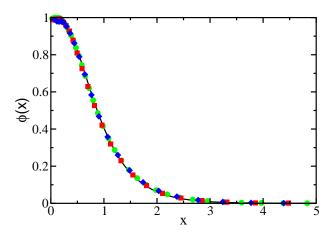We generated the steady state distribution by inject-

FIG. 7: The scaling function underlying the velocity distribution. The velocity distributions in figure 6 were normalized by the stationary distribution as in Eq. (28). The solid line is the theoretical scaling function (35).

FIG. 8: The cut-off velocity $V(t)$ as a function of time t (circles). The solid line is a fit to Eq. (27). Also shown is a broken line with slope -1.

ing energy at a fixed rate. This was done by uniformly removing particles from the distribution and re-injecting them according to a Gaussian distribution with a large characteristic velocity. Once the system reaches a steady state, we turn off the energy injection and observe the distribution $f(v,t)$ as it cools.

Figure 6 shows the driven steady-state distribution and the freely cooling distributions at three later times. The results verify that the steady-state has a power-law tail, $f_s(v) \sim v^{-3}$ and that the freely cooling distributions are close to the steady-state distribution for sufficiently small velocities. Figure 7 shows the same three time-dependent distributions divided by the steady distribution as in Eq. (28) and rescaled by the cut-off velocity $V(t)$ to collapse the data onto the theoretical prediction (35).

The time dependence of the cut-off velocity, given by Eq. (26), holds until V is order $v_0 \equiv 1$. Thus, the life-time of the collapsing power-law solution approaches a constant of order unity as $V(0)$ becomes infinite. During most of the time that the power-law is collapsing, V decays algebraically with time, $V(t) \sim t^{-1/\lambda}$. Figure 8 shows the cut-off velocity versus time together with a fit to the form (27) with $\lambda = 1$. We also checked that the tail of the cooling distribution is exponential. We conclude that for completely inelastic hard-spheres, the simulation results are in excellent agreement with the theoretical predictions.

VII. SUMMARY

In summary, we have found a new class of stationary solutions, driven steady-state, and time-dependent states for inelastic gases. These states are completely general: they exist in arbitrary dimension for arbitrary collision rates including both hard spheres and Maxwell molecules.
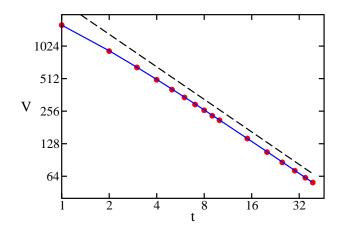
In the nonequilibrium steady-states, energy is injected at large velocities, it cascades down to small velocities, and it is dissipated over a power-law range. Generically, the steady-state distributions have a power-law high-energy tail. The characteristic exponents were obtained analytically and they vary with the spatial dimension and the collision rules. Formally, the stationary solutions are characterized by an infinite dissipation rate, while the energy density may be either finite or infinite. In an actual particle system, these steady-states may be realized only up to the energy injection scale, so that all thermodynamic characteristics including the dissipation rate and the energy density are finite.

When energy injection is turned-off, the velocity distribution is time independent only in a shrinking range of velocities and it decays sharply as a stretched exponential at large velocities. For completely inelastic collisions, the scaling function underlying this behavior can be obtained exactly from the linearized Boltzmann equation and at small velocities, there is a subtle log-normal correction to the power-law behavior. Although we analyzed only the one-dimensional case, we expect the same behavior in higher-dimension. These time-dependent states can be loosely thought of as a hybrid between the stationary solution and the well-known, freely-cooling solution. Both the time-dependence of the characteristic velocity and the decay at large velocities are similar, but not identical, to those occurring for freely cooling granular gases.

In the typical vigorous driving or shaking experiments, energy is injected at all scales. Theoretically, these steady-states are modeled by adding an explicit forcing term to the Boltzmann equation. The nonequilibrium steady-states found here are different in several ways. They require a separation of scales with energy injected at large scales only and most particles having a much smaller energy. Moreover, the steady states are universal, as they do not depend on the precise nature of the injection mechanism, as long as it is limited to high-energies. The other condition is that the dynamics be purely col-

lisional.

Inelastic cascades are a direct consequence of the collision rule. Dynamics of energetic particles follow a linear equation, that may be valid beyond the range of applicability of the full nonlinear kinetic theory. Given this generality, we propose that steady state distributions may be achieved in driven granular gas experiments where energy is injected at very large velocity scales [48]. Precisely how to realize these steady-states is an open challenge. One plausible scenario is constant injection of high-energy particles into a very large granular medium. In this set-up, the energy injection is limited to high-energy scale. Having a very large system diminishes the role of the boundary and ensures that the dynamics are collisional.

Cascade processes occur in many other physical systems. The inelastic cascade process for one-dimensional hard-spheres is identical to that found for the grinding process in Ref. [47], and in both problems $\sigma = 3$. Indeed, the cascade process (6) is equivalent to a fragmentation process. In fluid turbulence, the fluid is forced at a large spatial scale, energy cascades from large scales to small scales, where it is dissipated due to viscosity [49]. The situation found here for granular gases is analogous to wave turbulence, that is described by a kinetic theory for wave collisions [50]. One difference with the Kolmogorov spectra of fluid turbulence is that the characteristic exponents are irrational because they do not follow from dimensional analysis.

In closing, the kinetic theory of inelastic collisions is remarkable as the nonlinear Boltzmann equation admits a number of distinct solutions including a stationary solution, a transient solution, and a hybrid that interpolates between the two. Nonlinearity, nonlocality, and the lack of energy conservation are responsible for this remarkable complexity. We end with an open question: do other families of solutions exist?

Acknowledgments

[1] *Kinetic theory of granular gases*, N. Brilliantov and T. Pöschel, (Oxford, Oxford, 2003).

[2] *Granular Gases*, T. Pöschel and S. Luding (editors), (Springer, Berlin, 2000).

[3] *Granular Gas Dynamics*, T. Pöschel and N. Brilliantov (editors), (Springer, Berlin, 2003).

[4] W. Losert, D. G. W. Cooper, J. Delour, A. Kudrolli, and J. P. Gollub, Chaos **9**, 682 (1999).

[5] F. Rouyer and N. Menon, Phys. Rev. Lett. **85**, 3676 (2000)

[6] I. S. Aranson and J. S. Olafsen Phys. Rev. E **66**, 061302 (2002).

[7] Y. Du, H. Li, and L. P. Kadanoff, Phys. Rev. Lett. **74**, 1268 (1995).

[8] A. Kudrolli, M. Wolpert and J. P. Gollub, Phys. Rev. Lett. **78**, 1383 (1997).

[9] E. L. Grossman, T. Zhou, and E. Ben-Naim, Phys. Rev. E **55**, 4200 (1997).

[10] R. D. Wildman and D. J. Parker, Phys. Rev. Lett. **88**, 064301 (2002).

[11] K. Feitosa and N. Menon, Phys. Rev. Lett. **88**, 198301 (2002).

[12] E. Ben-Naim, S. Y. Chen, G. D. Doolen, and S. Redner, Phys. Rev. Lett. **83**, 4069 (1999).

[13] E. C. Rericha, C. Bizon, M. D. Shattuck, and H. L. Swinney, Phys. Rev. Lett. **88**, 014302 (2002).

[14] A. Samadani, L. Mahadevan, and A. Kudrolli, J. Fluid Mech. **452**, 293 (2002).

[15] S. McNamara and W. R. Young, Phys Fluids A **4**, 496 (1992).

[16] J. S. Olafsen and J. S. Urbach, Phys. Rev. Lett. **81**, 4369 (1998).

[17] S. Luding and H. J. Herrmann, Chaos **9**, 673 (1999).

[18] X. Nie, E. Ben-Naim, and S. Y. Chen, Phys. Rev. Lett. **89**, 204301 (2002).

[19] D. van der Meer, K. van der Weele, and D. Lohse, Phys. Rev. Lett **88**, 174302 (2002).

[20] I. Goldhirsch, and G. Zanetti, Phys. Rev. Lett. **70**, 1619 (1993).

[21] E. Khain and B. Meerson, Europhys. Lett. **65**, 193 (2004).

[22] J. T. Jenkins and M. W. Richman, Phys. Fluids **28**, 3485 (1985).

[23] J. J. Brey, J. W. Dufty, C. S. Kim, and A. Santos, Phys. Rev. E **58**, 4638 (1998).

[24] J. Lutsko, J. J. Brey, and J. W. Dufty, Phys. Rev. E **65**, 051304 (2002).

[25] I. Goldhirsch, Ann. Rev. Fluid. Mech. **35**, 267 (2003).

[26] K. Kohlstedt, A. Snezhko, M. V. Sapoznikov, I. S. Aranson, J. S. Olafsen, and E. Ben-Naim, preprint.

[27] T. P. C. van Noije and M. H. Ernst, Gran. Matt. **1**, 57 (1998).

[28] E. Ben-Naim and J. Machta, Phys. Rev. Lett. **94**, 138001 (2005).

[29] P. Résibois and M. de Leener, *Classical Kinetic Theory of Fluids* (John Wiley, New York, 1977).

[30] C. Sire and P. L. Krapivsky, Phys. Rev. Lett. **86**, 2494 (2001).

[31] J. C. Maxwell, Phil. Trans. R. Soc. **157**, 49 (1867).

[32] C. Truesdell and R. G. Muncaster, *Fundamentals of Maxwell's Kinetic Theory of a Simple Monoatomic Gas* (Academic Press, New York, 1980).

[33] M. H. Ernst, Phys. Reports **78**, 1 (1981).

[34] A. V. Bobylev, Sov. Sci. Rev. C. Math. Phys. **7**, 111 (1988).

[35] S. E. Esipov and T. Pöschel, J. Stat. Phys. **86**, 1385 (1997).

[36] J .J. Brey, J. W. Dufty, and A. Santos, J. Stat. Phys. **87**,

1051 (1997).

[37] P. K. Haff, J. Fluid Mech. **134**, 401 (1983).

[38] I. S. Gradshteyn and I. M. Ryzhik, *Table of Integrals, Series, and Products*, (Academic Press, New York, 1972).

[39] A. V. Bobylev and C. Cercignani, J. Stat. Phys. **106**, 1039 (2002).

[40] E. Ben-Naim and P. L. Krapivsky, Lect. Notes. in Phys. **624**, 63 (2003).

[41] A. Santos and M. H. Ernst, Phys. Rev. E 68, 011305 (2003)

[42] T. Antal, M. Droz, and A. Lipowski, Phys. Rev. E **66**, 062301 (2002).

[43] P. L. Krapivsky and E. Ben-Naim, J. Phys. A **35**, L147 (2002).

[44] E. Ben-Naim and P. L. Krapivsky, Phys. Rev. E **66**, 011309 (2002).

[45] M. H. Ernst and R. Brito, Europhys. Lett. **58**, 182 (2002).

[46] M. H. Ernst and R. Brito, J. Stat. Phys. **109**, 407 (2002).

[47] E. Ben-Naim and P.L. Krapivsky Phys. Lett. A **275**, 48 (2000).

[48] Algebraic tails with exponents comparable with these reported here were observed recently in sheared granular layers, S. Moka and P. R. Nott, cond-mat/0412506.

[49] U. Frisch, *Turbulence: The legacy of A. N. Kolmogorov* (Cambridge University Press, New York, 1995).

[50] V. E. Zakharov, V. S. Lvov, and G. Falkovich, *Kolomogorov Spectra of Turbulence I: Wave Turbulence* (Springer-Verlag, New York, 1992).

[51] R. S. Krupp, *A nonequilibrium solution of the Fourier transformed Boltzmann equation*, M.S. Thesis, MIT (1967); *Investigation of solutions to the Fourier transformed Boltzmann equation*, Ph.D. Thesis, MIT (1970).

[52] E. Ben-Naim and P. L. Krapivsky, Phys. Rev. E **61**, R5 (2000).

[53] D. ben-Avraham, E. Ben-Naim, K. Lindenberg, and A. Rosas, Phys. Rev. E **68**, 031104 (2003).

[54] R. Lambiotte and L. Brenig, unpublished.

APPENDIX A: EXACT SOLUTION FOR ONE-DIMENSIONAL MAXWELL MOLECULES

The stationary velocity distribution can be obtained analytically for one-dimensional Maxwell molecules. Since the governing equation (3) is in a convolution form, it is natural to employ the Fourier transform [51], $F(k) = \int dv\, e^{ikv} f(v)$. The stationary state $(\partial/\partial t \equiv 0)$ satisfies the non-local and non-linear equation [52, 53]

$$F(k) = F(pk)F(qk). \tag{A1}$$

Normalization implies $F(0) = 1$.

For elastic collisions, $p = 0$, every distribution is a stationary state, but this is a one-dimensional anomaly, because in higher dimensions, the stationary distribution is always Maxwellian [31]. For all $0 \le p \le 1$ and $p+q = 1$, there is a family of stationary solutions

$$F(k) = \exp\left(-v_0|k|\right), \tag{A2}$$

characterized by the arbitrary typical velocity v_0. Performing the inverse Fourier transform, the velocity distribution is a Lorentz (Cauchy) distribution [54]

$$f(v) = \frac{1}{\pi v_0} \frac{1}{1 + (v/v_0)^2}. \tag{A3}$$

This distribution decays algebraically at large velocities in agreement with (17).